42nd AIAA Aerospace Sciences Meeting and Exhibit
January 5-8, 2004, Reno, NV

Paper 2004-1033

THERMODYNAMIC ANALYSIS OF COMBUSTION PROCESSES FOR PROPULSION SYSTEMS

E. Wintenberger and J. E. Shepherd
Graduate Aeronautical Laboratories,
California Institute of Technology, Pasadena, CA 91125

A key issue in conceptual design and analysis of proposed propulsion systems is the role of the combustion mode in determining the overall efficiency of the system. Of particular recent interest are detonations and the efficiency of detonation-based propulsion systems as compared to more conventional systems based on low-speed flames. Our goal is to understand, based on thermodynamics, the merits of detonative combustion relative to deflagrative combustion characteristic of conventional ramjet and turbojet engines. After reviewing detonation thermodynamics, we analyze the merits of detonations for steady flow systems and highlight the importance of the irreversible portion of the entropy rise in steady flow analysis. The conventional analysis of steady combustion waves is reformulated to obtain solutions at a fixed stagnation enthalpy. The implications of this analysis are that detonations are less desirable than deflagrations for a steady air-breathing combustion system since they entail a greater entropy rise at a given flight condition. This leads us to consider the situation for unsteady, i.e., intermittent or pulsed, combustion systems which use various modes of operation. For unsteady detonation waves, we consider a notional cyclic process for a closed system (the Fickett-Jacobs cycle) in order to circumvent the difficulties associated with analyzing a system with time-dependent and spatially inhomogeneous states. We use the thermodynamic principles for closed systems to compute the maximum amount of mechanical work produced by a cycle using an unsteady detonation process. This ideal mechanical work is used to compute a thermal efficiency for detonations. Although this efficiency cannot be precisely translated into propulsive efficiency, the results are useful in comparing detonations with other combustion modes. We find that the efficiency of cycles based on detonation and constant-volume combustion are very similar and superior to a constant-pressure combustion (Brayton) cycle when compared on the basis of pressure at the start of the combustion process.

Nomenclature

A	piston area
C_p	specific heat capacity at constant pressure
E	total energy
e	internal energy per unit mass
F	thrust
h	enthalpy per unit mass
M	Mach number
M_{CJ}	Chapman-Jouguet detonation Mach number
$\mathcal{M}$	mass of explosive in closed system
$\dot{m}$	mass flow rate
P	pressure
P_t	total pressure
Q	heat exchange
q_c	mixture specific heat of combustion
q_{in}	cycle heat addition per unit mass
q_{out}	cycle heat removal per unit mass
R	perfect gas constant
s	entropy per unit mass
T	temperature
T_t	total temperature
t	time
U_{CJ}	Chapman-Jouguet detonation velocity
u	flow velocity in fixed reference frame
u'	flow velocity in wave reference frame
u_p	piston velocity
v	specific volume
W	work
w	work per unit mass
w_{net}	net work done per unit mass during cycle
γ	specific heat ratio
Δs_{min}	minimum part of entropy rise
Δs_{irr}	irreversible part of entropy rise
ϕ	equivalence ratio
π_c	compression ratio $= P_{1'}/P_1$
π_c'	combustion pressure ratio $= P_2/P_1$
ρ	density
η_{FJ}	FJ cycle thermal efficiency
η_{th}	thermal efficiency

Copyright © 2004 by California Institute of Technology. Published by the American Institute of Aeronautics and Astronautics, Inc. with permission.

Introduction

The thermodynamic processes encountered in air-breathing propulsion involve sequential compression, combustion, and expansion. This sequence is turned into a closed cycle through a constant pressure process during which the fluid exhausted into the atmosphere at the end of the expansion process is converted into the inlet fluid by exchanging heat and work with the surroundings. The thermal efficiency of an arbitrary cycle involving adiabatic combustion can be defined as the ratio of the work done by the system to the specific heat of combustion of the mixture.

$$\eta_{th} = \frac{w}{q_c} \tag{1}$$

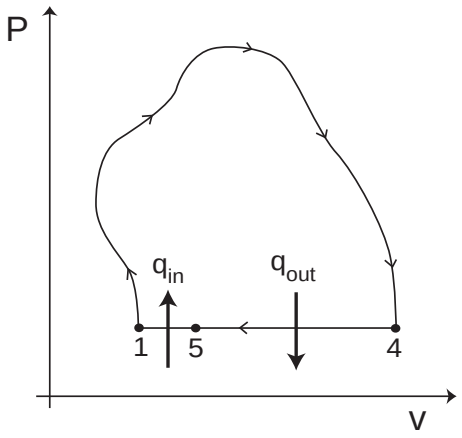

Fig. 1 Arbitrary thermodynamic cycle ending with constant-pressure process.

The work done and mixture heat of combustion can be clarified by considering a thermodynamic cycle consisting of an arbitrary adiabatic process taking the system from its initial state 1 to state 4, and ending with a constant pressure process taking the system back to state 1. As shown in Fig. 1, there is an intermediate state 5 between 4 and 1. The heat interaction between steps 4 and 5 is required to remove an amount of thermal energy $q_{out} > 0$ from the products of combustion and cool the flow down from the exhaust temperature to the ambient conditions. Since this process occurs at constant pressure, the heat interaction can be determined from the enthalpy change

$$q_{out} = h_4 - h_5 \ . \tag{2}$$

The heat interaction between steps 5 and 1 is required to add an amount of thermal energy $q_{in} > 0$ in order to convert the combustion products back to reactants. This interaction also takes place at constant pressure so that

$$q_{in} = h_1 - h_5 \ . \tag{3}$$

Note that this defines the quantity $q_c = q_{in}$ in a fashion consistent with standard thermochemical practice if the ambient conditions correspond to the thermodynamic standard state. Applying the First Law of Thermodynamics around the cycle, the work done by the system can be computed as

$$w = q_{in} - q_{out} = h_1 - h_4 \ . \tag{4}$$

The thermal efficiency can, therefore, be written as

$$\eta_{th} = \frac{h_1 - h_4}{h_1 - h_5} = \frac{h_1 - h_4}{q_c} \tag{5}$$

which agrees with the definition given in Eq. 1 in terms of the mixture specific heat of combustion.

For steady flow engines, the cycle analysis based on a closed system (fixed mass of material) is completely equivalent to the flow path analysis based on an open system, as long as the mass and momentum contributions of the fuel are negligible and the exhaust flow is fully expanded at the exit plane.[1] Within these assumptions, we can make a correspondence between states in the cyclic process of Fig. 1 and an open thermodynamic cycle. If the states in the open and closed cycles are equivalent, then the thermal efficiencies are the same for the two processes. The equivalence is based on the control volume analysis of the energy balance in an open system whose inlet plane is at state 1 and exit plane is at state 4.

$$h_1 + u_1^2/2 = h_4 + u_4^2/2 \tag{6}$$

Using the cycle thermal efficiency as defined in Eq. 1, we find that

$$\eta_{th} = \frac{u_4^2 - u_1^2}{2q_c} \ . \tag{7}$$

Based on this equivalence, the thrust of a steady pressure-matched propulsion system can be directly calculated from the thermal efficiency.[1]

$$F = \dot{m}_1 \left(u_4 - u_1\right) = \dot{m}_1 \left(\sqrt{u_1^2 + 2\eta_{th} q_c} - u_1\right) \tag{8}$$

This method can be extended to unsteady propulsion systems when the average exit plane pressure equals the ambient pressure.[1] However, for unsteady flow, the thrust calculation with the cycle approach requires the explicit computation of efficiency for the unsteady cycle and the knowledge of another parameter, called the efficiency of non-uniformity by Foa.[1] These calculations require detailed experimental measurements, unsteady analytical models, or numerical simulations.

For an ideal (reversible) process, the heat removed during the constant-pressure process 4–5 can be expressed as

$$q_{out} = \int_{s_5}^{s_4} T ds \tag{9}$$

and the thermal efficiency is

$$\eta_{th} = 1 - \frac{\int_{s_5}^{s_4} T ds}{q_c} \ . \tag{10}$$

For a given initial state 1 and a given mixture, state 5 is fixed and the value of the entropy is determined by the specific heat of combustion and the product and reactant composition. Thus, the heat removed q_{out} increases and the thermal efficiency decreases with increasing values of s_4. In general, the thermal efficiency is maximized when the entropy rise during process 1–4 is minimized.

This general result can be computed explicitly if we consider a perfect gas and take $s_5 = s_1$, which is approximately satisfied for real mixtures and exactly so for the simple model discussed later in this paper. The integral of Eq. 9 is calculated explicitly as a function of the entropy rise between states 1 and 4, and the thermal efficiency becomes

$$\eta_{th} = 1 - \frac{C_p T_1}{q_c}\left[\exp\left(\frac{s_4 - s_1}{C_p}\right) - 1\right] . \qquad (11)$$

The overall entropy rise is the sum of the entropy rise generated by combustion and of the entropy increments generated by irreversible processes such as shocks, friction, heat transfer, Rayleigh losses (combustion or equivalent heat addition at finite Mach number), or fuel-air mixing.[1] The entropy increment associated with the combustion process is often the largest of all increments in the cycle. A portion of this entropy increment is associated with the fact that the temperature increases significantly in combustion, analogous to the entropy increase that is produced by a reversible addition of heat to a non-flowing system. However, there is also an irreversible component, which depends on the combustion mode. Because of the dependence of the thermal efficiency on the total entropy rise, the selection of the combustion mode is critical to engine performance.

Entropy variation along the Hugoniot

In this section, we supply the well-known and basic facts regarding the elementary gas dynamics and thermodynamics of detonation waves considered as discontinuities. The different steady combustion modes that can be obtained are usually analyzed using a control volume surrounding the combustion wave, such as that of Fig. 2. The mass, momentum, and energy conservation equations are applied for steady, constant-area, and inviscid flow.

$$\rho_1 u_1' = \rho_2 u_2' \qquad (12)$$

$$P_1 + \rho_1 {u_1'}^2 = P_2 + \rho_2 {u_2'}^2 \qquad (13)$$

$$h_1 + {u_1'}^2/2 = h_2 + {u_2'}^2/2 \qquad (14)$$

States 1 and 2 correspond respectively to the reactants upstream of the wave and the products downstream of the wave. The usual analysis considers fixed thermodynamic conditions upstream (P_1, ρ_1, h_1) and a variable inflow velocity u_1'. Although this is the conventional approach, as we will see later, it is not the appropriate approach for optimizing steady, air-breathing propulsion systems. From Eqs. 12–14, the Hugoniot relationship can be obtained

$$h_2 - h_1 = \frac{1}{2}(P_2 - P_1)(1/\rho_1 + 1/\rho_2) . \qquad (15)$$

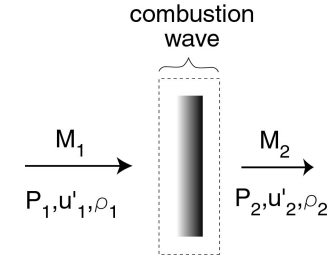

Fig. 2 Control volume used to analyze steady combustion waves.

The Hugoniot curve determines the locus of the possible solutions for state 2 from a given state 1 and a given energy release q_c. In particular, it is instructive to plot the Hugoniot on a pressure-specific volume diagram (Fig. 3). The solution for state 2 must also fall on the Rayleigh line, which is given by

$$P_2 - P_1 = -(\rho_1 u_1')^2(1/\rho_2 - 1/\rho_1) . \qquad (16)$$

For a given state 1 and velocity u_1', the solution to state 2 is found by simultaneously solving Eqs. 15 and 16, i.e., the solution is given by the intersection of the Hugoniot and the Rayleigh line. From Eq. 16, we can show that the dashed portion of the curve labeled "forbidden" in Fig. 3 is physically impossible since the values of $\rho u'$ are imaginary there. The solutions located in the upper branch of the Hugoniot represent supersonic waves (detonations), whereas the solutions located in the lower branch correspond to subsonic waves (deflagrations).

The points where the Rayleigh line is tangent to the Hugoniot curve are called the Chapman-Jouguet (CJ) points. There are two CJ points, the upper CJ point (CJ_U) located on the detonation branch and the lower CJ point (CJ_L) located on the deflagration branch. The CJ points are characterized by sonic flow downstream of the combustion wave and correspond to entropy extrema of the burned gases. It is possible to show, based on the curvature of the Hugoniot curve, that the entropy is minimum at the upper CJ point and maximum at the lower CJ point.[2]

The solution to Eqs. 12–14 is uniquely determined only with some additional considerations. For deflagrations, the structure of the combustion wave and turbulent and diffusive transport processes determine the actual propagation speed. For detonations, gas dynamic considerations are apparently sufficient to determine the propagation speed (corresponding to the CJ_U solution), independent of the actual structure of the wave.[2] The CJ points divide the possible locus

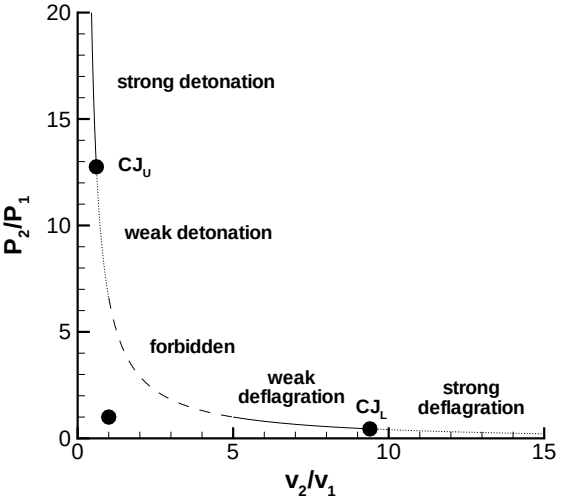

Fig. 3 Hugoniot curve for a perfect gas with γ=1.4 and q_c/C_pT_1=4.

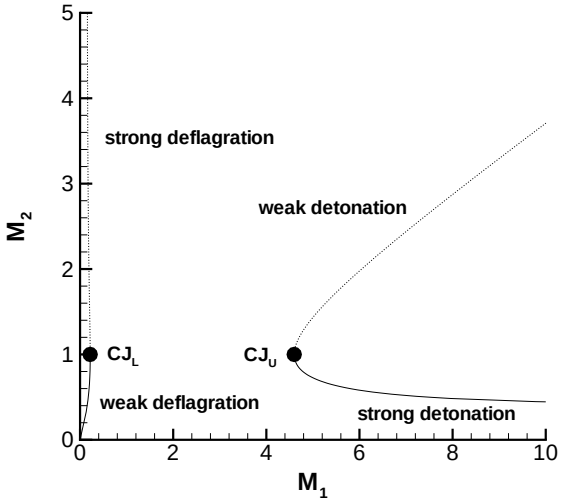

Fig. 4 Solutions of the conservation equations for the Hugoniot for M_2 as a function of M_1, γ=1.4, q_c/C_pT_1=4.

of solutions into four regions, corresponding to strong detonations (supersonic flow to subsonic), weak detonations (supersonic to supersonic), weak deflagrations (subsonic to subsonic), and strong deflagrations (subsonic to supersonic). Strong deflagrations and weak detonations can be ruled out except in extraordinary situations by considering the reaction zone structure. The physically acceptable and observed solutions for steady waves are weak deflagrations and strong detonations. For deflagrations, there is no unique solution from a gas dynamic view point and other processes, such as turbulence and molecular diffusion, have to be considered. For detonations, there is one special solution, $\mathrm{CJ_U}$, that is singled out from a thermodynamic point of view. Strong detonations are observed only in the transient state or if there is an "effective" piston created by the flow following the wave.

We now consider the case of the perfect gas $P = \rho RT$ in order to numerically illustrate the previous points. We will assume equal specific heat capacities for reactants and products

$$C_p = \frac{\gamma}{\gamma - 1} R \tag{17}$$

and the enthalpy in the reactants and products can be expressed as

$$h_1 = C_p T_1 \qquad h_2 = C_p T_2 - q_c \, . \tag{18}$$

The set of Eqs. 12–14 can be rewritten for a perfect gas as a function of the Mach numbers upstream and downstream of the wave.

$$\frac{\rho_2}{\rho_1} = \frac{M_1^2(1+\gamma M_2^2)}{M_2^2(1+\gamma M_1^2)} \tag{19}$$

$$\frac{P_2}{P_1} = \frac{1+\gamma M_1^2}{1+\gamma M_2^2} \tag{20}$$

$$\frac{q_c}{C_pT_1} + 1 + \frac{\gamma-1}{2}M_1^2 = \frac{M_2^2(1+\gamma M_1^2)^2}{M_1^2(1+\gamma M_2^2)^2}\left(1+\frac{\gamma-1}{2}M_2^2\right) \tag{21}$$

This set of equations can be solved analytically for a given q_c and initial state. The Mach number downstream of the wave M_2 is plotted as a function of the Mach number upstream of the wave M_1 in Fig. 4. The lower CJ point yields the highest deflagration Mach number, while the upper CJ point corresponds to the lowest detonation Mach number.

The entropy rise associated with the combustion process can be computed from Eqs. 19 and 20.

$$\frac{s_2 - s_1}{R} = \frac{\gamma}{\gamma - 1} \ln\left(\frac{T_2}{T_1}\right) - \ln\left(\frac{P_2}{P_1}\right) \tag{22}$$

The entropy rise is plotted in Fig. 5 as a function of the specific volume. The different solution regions are shown and the entropy rise is minimum at the CJ detonation point and maximum at the CJ deflagration point. Thus, from Eq. 11, it appears as if a cycle using detonation combustion will yield the highest thermal efficiency since it has the lowest entropy rise.

The role of irreversibility

The fact that the entropy rise is minimum at the CJ detonation point, in conjunction with the result of Eq. 10, has motivated several efforts to explore detonation applications to steady flow propulsion.[3–5]

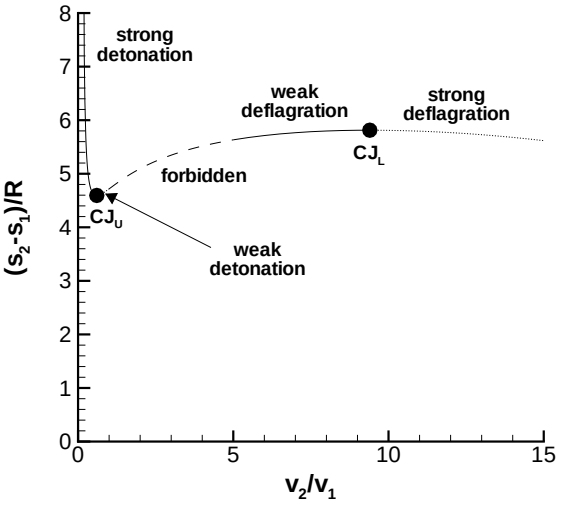

Fig. 5 Variation of the total entropy rise along the Hugoniot, γ=1.4, q_c/C_pT_1=4.

However, in spite of the apparent lower entropy rise generated by detonations as compared with deflagrations, these studies concluded that the performance of steady detonation-based engines is systematically and substantially lower than that of the ramjet.

The explanation of this apparent contradiction lies in considering the role of entropy generation and irreversible processes in the combustor. It is a general conclusion of thermodynamics and can be explicitly shown using availability arguments[6] that the work obtained is maximized when the irreversibility is minimized. When portions of the propulsion system involve losses and irreversible generation of entropy, the efficiency is reduced and the reduction in performance (specific thrust) can be directly related to the irreversible entropy increase.[7]

The entropy rise occurring during premixed combustion in a flowing gas has a minimum component due to the energy release and the chemical reactions, and an additional, irreversible, component due to the finite velocity and, in the case of a detonation, the leading shock wave.

$$s_2 - s_1 = \Delta s_{min} + \Delta s_{irr} \tag{23}$$

For a combustion wave such as Fig. 2, we propose that the minimum entropy rise (for a *fixed* upstream state and velocity) can be computed by considering the ideal stagnation or total state.* The total properties at a point in the flow are defined as the values obtained by isentropically bringing the flow to rest. For example, the total enthalpy is

$$h_t = h + \frac{u^2}{2} \tag{24}$$

and the total pressure and temperature are defined by

$$h(P_t, s) = h_t \qquad h(T_t, s) = h_t \tag{25}$$

where by definition $s_t = s$. The process of computing the stagnation state is illustrated graphically in the (h,s) or Mollier diagram of Fig. 6. At fixed total enthalpy, the total pressure decreases with increasing entropy

$$dP_t = -\rho_t T_t ds \tag{26}$$

so that the minimum entropy rise is associated with the highest total pressure, which is the upstream value P_{t1}. This is illustrated graphically in Fig. 6, showing the additional entropy increment Δs_{irr} associated with a total pressure decrement $P_{t1} - P_{t2}$.

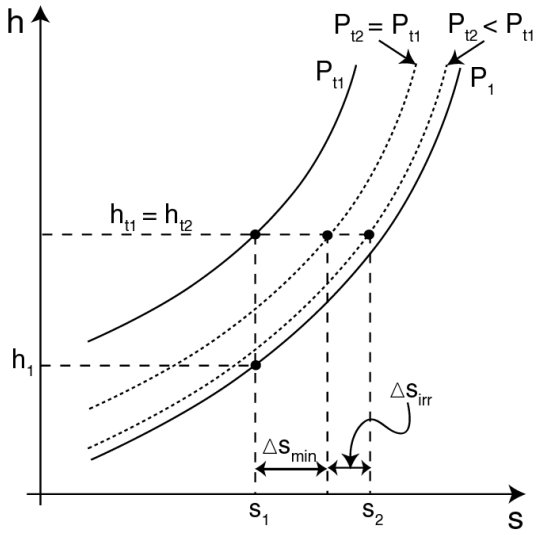

Fig. 6 Mollier diagram for constant-pressure combustion. Solid lines are isobars for reactants and dotted lines are isobars for products.

For a given stagnation state, the minimum entropy rise can be determined for gas mixtures with realistic thermochemistry by considering an ideal constant-pressure (zero velocity) combustion process. The first step is to determine the total temperature in the products from the energy balance equation

$$h_2(T_{t2}) = h_1(T_{t1}) \tag{27}$$

where the species in state 2 are determined by carrying out a chemical equilibrium computation. The second step is to determine the entropy rise across the combustion wave by using the stagnation pressures, temperatures, and compositions to evaluate the entropy for reactants and products

$$\Delta s_{min} = s_2(T_{t2}, P_{t1}) - s_1(T_{t1}, P_{t1}) \; . \tag{28}$$

*This conjecture is easy to demonstrate for a perfect gas with an effective heat addition model of combustion, for example, see Oates,[8] p. 44. We also demonstrate the correctness of this idea explicitly in subsequent computations for the one-γ detonation model and numerical solutions with realistic thermochemistry.

The total entropy jump across the wave is

$$s_2 - s_1 = s_2(T_2, P_2) - s_1(T_1, P_1) \tag{29}$$

where state 2 in the products is determined by solving the jump conditions. The irreversible component can then be computed by using Eq. 23.

For a perfect gas model, the entropy change can be explicitly computed as

$$s_2 - s_1 = C_p \ln\left(\frac{T_{t2}}{T_{t1}}\right) - R \ln\left(\frac{P_{t2}}{P_{t1}}\right) . \tag{30}$$

From Eq. 28, the minimum entropy rise is

$$\Delta s_{min} = C_p \ln\left(\frac{T_{t2}}{T_{t1}}\right) \tag{31}$$

and the irreversible component is

$$\Delta s_{irr} = -R \ln\left(\frac{P_{t2}}{P_{t1}}\right) . \tag{32}$$

The minimum component can be identified as the amount of entropy increase that would occur with an equivalent *reversible* addition of heat

$$ds = \frac{dq}{T} \tag{33}$$

at constant pressure, for which

$$dq = dh = C_p dT . \tag{34}$$

Substituting and integrating from stagnation state 1 to 2, we find that

$$\Delta s_{rev} = C_p \ln\left(\frac{T_{t2}}{T_{t1}}\right) \tag{35}$$

which is identical to the expression for the minimum entropy rise found from evaluating the entropy change using the prescription given above. In what follows, we will also refer to the minimum entropy rise as the *reversible* entropy rise. Using these definitions, we show in Fig. 7 the partition of the entropy into these two portions for the one-γ model of detonation considered earlier.

Although the total entropy rise is lower for the detonation branch than the deflagration branch, a much larger portion (greater than 50%) of the entropy rise is irreversible for detonations than for deflagrations (less than 5%). Separate computations show that the majority of the irreversible portion of the entropy rise for detonations is due to the entropy jump across the shock front, which can be obtained directly from the total pressure decrease across the shock wave and Eq. 30. This loss in total pressure is orders of magnitude larger for detonation than for deflagration solutions and was shown[5] to be responsible for the lower performance of detonation-based engines relative

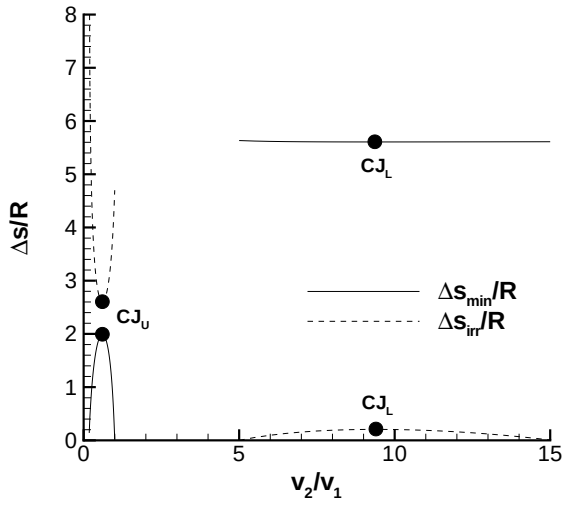

Fig. 7 Reversible and irreversible components of the entropy rise along the Hugoniot, γ=1.4, q_c/C_pT_1=4.

to the ramjet. Hence, the paradox mentioned earlier can be resolved by considering not just the total entropy rise, but by determining what part of this is irreversible. An alternative way to look at this issue is given in the next section, where we reformulate the jump conditions so that the role of irreversible entropy rise in the calculation of the thermal efficiency can be demonstrated explicitly.

Irreversible entropy rise and thermal efficiency

The role of the irreversible part of the entropy rise can be explored further by considering Eq. 10. In order to compare objectively different combustion modes, the engine has to be studied in a given flight situation for a fixed amount of energy release during the combustion, as shown in Fig. 8. Our notional engine consists of an inlet, a combustion chamber, and a nozzle.

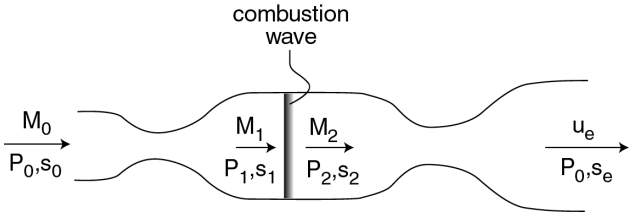

Fig. 8 Ideal steady engine in flight showing the location of the combustion wave.

The entropy rise between the inlet and exit planes is the sum of the entropy rise through the combustion and the irreversible entropy increments through the inlet and nozzle. Grouping together the irreversible entropy increments through the inlet, the combustion chamber, and the nozzle,

$$s_e - s_0 = \Delta s_{min} + \Delta s_{irr} . \tag{36}$$

The minimum part of the entropy rise during combustion is constant for a fixed energy release and a fixed stagnation state upstream of the wave. From the general principles of thermodynamics and consistent with Eq. 10, the highest efficiency is obtained with the minimum irreversibility for a given chemical energy release q_c.

This general statement can be shown explicitly for the case of the perfect gas. The minimum component of the entropy rise for the one-γ model is

$$\Delta s_{min} = C_p \ln\left(1 + \frac{q_c}{C_p T_{t1}}\right) . \tag{37}$$

Substituting Eq. 36 into Eq. 11, and using the result of Eq. 37, the thermal efficiency can be expressed as a function of the irreversible entropy rise

$$\eta_{th} = 1 - \frac{C_p T_0}{q_c}\left[\left(1 + \frac{q_c}{C_p T_{t1}}\right)\exp\left(\frac{\Delta s_{irr}}{C_p}\right) - 1\right] . \tag{38}$$

From Eq. 38, the highest efficiency is obtained for $\Delta s_{irr} = 0$

$$\eta_{th} < \eta_{th}(\Delta s_{irr} = 0) = 1 - \frac{T_0}{T_{t1}} , \tag{39}$$

which is the classical expression for the ideal Brayton cycle.

Consider an idealized version of our notional engine, for which the thermal efficiency is determined only by the irreversible entropy rise during combustion. In order to compare different combustion modes, we need to calculate the irreversible entropy rise for all the possible solutions to Eqs. 12–14. However, the result of Fig. 5 does not apply directly because the velocity of the initial state and, consequently, the total enthalpy are not constant for the conventional Hugoniot analysis. Instead, it is necessary to compute another solution curve corresponding to a fixed freestream stagnation state, which we will refer to as the stagnation Hugoniot.

The stagnation Hugoniot

The stagnation Hugoniot is the locus of the solutions to the conservation equations (Eqs. 12-14) for a given stagnation state upstream of the combustion wave. The initial temperature and pressure upstream of the wave vary with the Mach number M_1. We compute explicitly the stagnation Hugoniot for a perfect gas, based on Eqs. 19–21. Equation 21 has to be rewritten as a function of the parameter q_c/C_pT_{t1}, which has a fixed value for a given freestream condition.

$$1 + \frac{q_c}{C_p T_{t1}} = \frac{M_2^2(1+\gamma M_1^2)^2(1+\frac{\gamma-1}{2}M_2^2)}{M_1^2(1+\gamma M_2^2)^2(1+\frac{\gamma-1}{2}M_1^2)} \tag{40}$$

This equation can be solved analytically, and the solution for M_2 as a function of M_1 is plotted in Fig. 9. The solution curves are very similar to those of Fig. 4, with the CJ points yielding the maximum deflagration and minimum detonation Mach numbers. There is, however, a difference for the weak detonation branch. As $M_1 \to \infty$, M_2 asymptotes to a constant value instead of becoming infinite as for the Hugoniot.

$$M_2 \to \sqrt{\frac{1-(\gamma-1)\frac{q_c}{C_pT_{t1}} + \sqrt{1-(\gamma^2-1)\frac{q_c}{C_pT_{t1}}}}{\gamma(\gamma-1)\frac{q_c}{C_pT_{t1}}}} \tag{41}$$

This is due to the fact that the stagnation conditions at state 2 are fixed by the stagnation conditions at state 1 and the heat release. Detonation solutions are found to be possible only for

$$\frac{q_c}{C_p T_{t1}} < \frac{1}{\gamma^2 - 1} . \tag{42}$$

This condition is imposed by the requirement that $T_1 > 0$ which is necessary for the limiting value of Eq. 41 to be real. For higher values of q_c/C_pT_{t1}, the total enthalpy is not high enough to enable a steady detonation in the combustor for the given value of the heat release, and no steady solutions exist.[5]

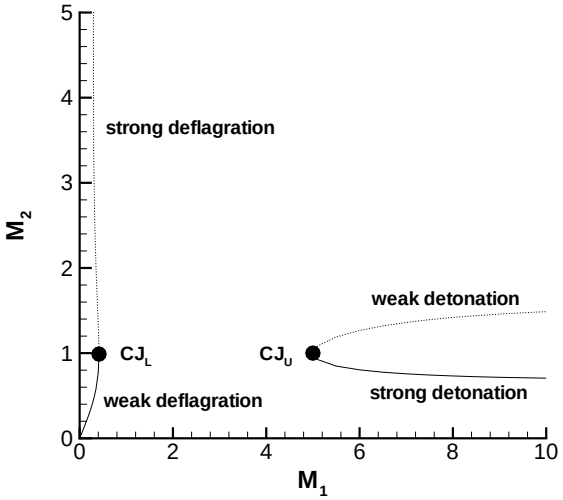

Fig. 9 Solutions of the conservation equations for the stagnation Hugoniot for M_2 as a function of M_1, γ=1.4, q_c/C_pT_{t1}=0.8.

For the conventional Hugoniot, Fig. 3, the entropy, pressure, and temperature at state 2 are finite for a constant-volume ($v_2 = v_1$) explosion process even though, in this limit, $M_1 \to \infty$. However, in the stagnation Hugoniot representation, the pressure ratio along the weak detonation branch becomes infinite as this limit is approached. As $M_1 \to \infty$, the static pressure at state 1 decreases towards zero because the total pressure is fixed, but the static pressure at state 2 remains finite due to the finite value of M_2. This explains the unusual shape of the stagnation Hugoniot,

which is plotted in the pressure-specific volume plane for γ=1.4 and q_c/C_pT_{t1}=0.8 in Fig. 10. Just as for the conventional Hugoniot, there is no solution in the positive quadrant of the pressure-specific volume plane for Rayleigh processes (Eq. 16). However, unlike the conventional Hugoniot, the stagnation Hugoniot curve is not continuous across this forbidden region. This means that the detonation and deflagration branches are disjoint.

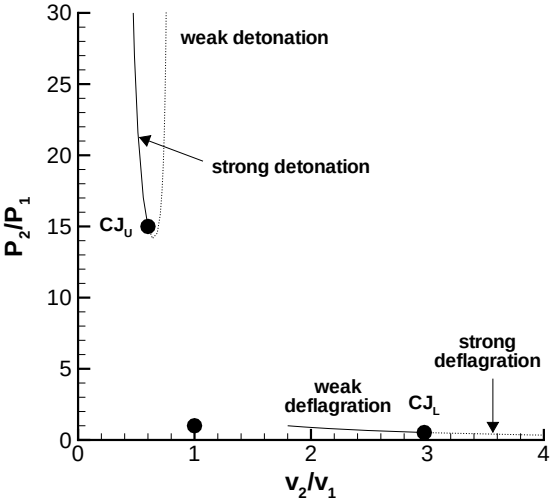

Fig. 10 Stagnation Hugoniot for a perfect gas with γ=1.4 and q_c/C_pT_{t1}=0.8.

The total entropy rise along the stagnation Hugoniot is shown in Fig. 11 as a function of the specific volume ratio. For a fixed heat release and initial stagnation state, the minimum entropy rise is constant (Eq. 37). As in the conventional Hugoniot, the CJ points correspond to extrema of the entropy. However, they are only local extrema because of the discontinuity of the solution curve in the pressure-specific volume plane. The CJ detonation point corresponds to a minimum in entropy along the detonation branch, while the CJ deflagration point corresponds to a maximum in entropy along the deflagration branch. However, the entropy rise associated with the CJ detonation point is much larger than that associated with the CJ deflagration point for all possible values of q_c/C_pT_{t1}. In general, the irreversible entropy rise associated with any physical solution on the deflagration branch is much lower than that for any detonation solution. Of all physically possible steady combustion modes, constant-pressure (CP) combustion at zero Mach number is the process with the smallest entropy rise for a fixed stagnation condition.

We now use the result of Eq. 39 to compare the thermal efficiency of ideal steady propulsion systems as a function of the combustion mode selected. Losses associated with shock waves, friction, mixing, or heat transfer are neglected, and the compression and ex-

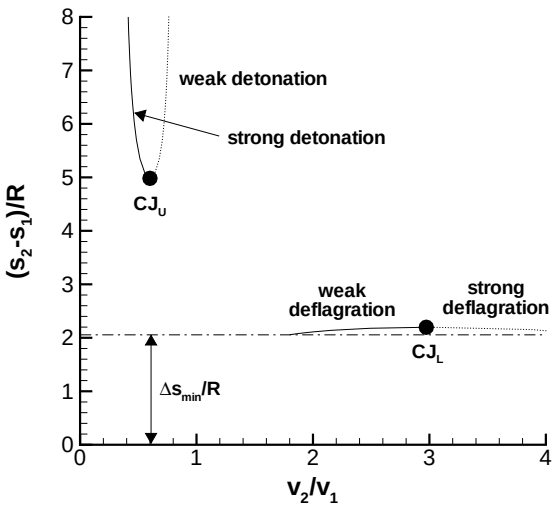

Fig. 11 Total entropy rise along the stagnation Hugoniot. The minimum component of the entropy rise is fixed along the stagnation Hugoniot and is shown as the straight line. The total entropy variation is due to the irreversible component only. γ=1.4, q_c/C_pT_{t1}=0.8.

pansion processes are assumed to be isentropic. The thermal efficiency for an ideal steady propulsion system flying at a Mach number of 5 is plotted in Fig. 12. The irreversible entropy rise in detonations strongly penalizes the efficiency of steady detonation-based engines compared to the conventional ideal ramjet. The values for the thermal efficiency at the upper CJ point obtained based on the stagnation Hugoniot are identical to those predicted by flow path analysis for ideal detonation ramjets.[5] Thus, this approach reconciles flow path analysis and thermodynamic cycle analysis for detonation ramjets. The values of the thermal efficiency of Fig. 12 are not representative of practical propulsion systems at a flight Mach number $M_0 = 5$ because the total temperature at the combustor outlet is too high to be sustained by the chamber walls. More realistic studies limit the total temperature at the combustor outlet based on material considerations, which decreases substantially the thermal efficiency.[5] The analysis of steady detonation-based ramjets also has to take into account effects such as condensation or auto-ignition of the fuel-air mixture and limitations associated with fuel sensitivity to detonation.[5] The net effect is that propulsion systems based on *steady* detonation waves have a very small thrust-producing range[5] and the maximum performance is always substantially lower than conventional turbojets or ramjets.[5]

For our ideal propulsion system, the CP combustion process yields the highest thermal efficiency of all physical solutions to the conservation equations. Foa[9] concluded that CP combustion was always the optimum solution for steady flow using an argument based

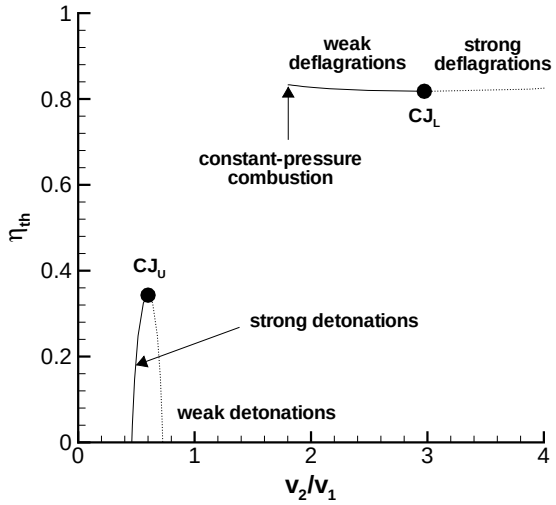

Fig. 12 Thermal efficiency of an ideal engine flying at $M_0 = 5$ as a function of the combustion mode selected, γ=1.4, $q_c/C_pT_{t1} = 0.8$.

on a polytropic approximation of the combustion mode for the perfect gas. We have now extended his result to all physically possible steady combustion modes. However, in order to compare practical propulsion systems based on different combustion modes, one also has to compute the irreversible entropy rise through the other components of the engine. The entropy rise associated with irreversible processes such as shocks, friction, mixing, or heat transfer may become significant[7] and dominate the results, particularly at high supersonic flight Mach numbers.

Detonation applications in unsteady flow: the Fickett-Jacobs cycle

The entropy minimum corresponding to CJ detonations and its implications on the thermal efficiency have also motivated significant efforts to apply unsteady detonations to propulsion, in particular through the research on pulse detonation engines.[10] Unsteady detonations can be analyzed on a thermodynamic basis by considering a closed system. The Fickett-Jacobs (FJ) cycle is a conceptual thermodynamic cycle that can be used to compute an upper bound to the amount of mechanical work that can be obtained from detonating a given mass of explosive. The advantage of the FJ cycle is that it provides a simple conceptual framework for handling detonations in a purely thermodynamic fashion, avoiding the complexity of unsteady gas dynamics[11,12] of realistic pulse detonation or pulsejet engines.

Basic FJ cycle

The FJ cycle for detonations is described in Fickett and Davis[13] (p. 35–38) and is an elaboration of the original ideas of Jacobs.[14] The notion of applying thermodynamic cycles to detonation was independently considered by Zel'dovich[15] 15 years before Jacobs, but Zel'dovich's ideas were not known† to Jacobs or Fickett and, until recently, there was no appreciation in the West of this work by Zel'dovich.

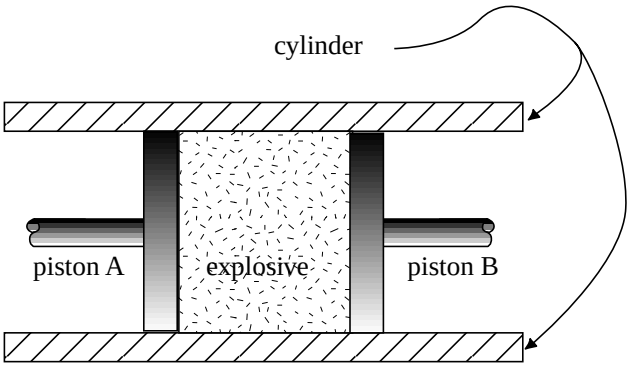

Fig. 13 Piston cylinder arrangement used to implement Fickett-Jacobs cycle.

The idea of the FJ cycle is similar to standard thermodynamic cycles such as the Otto and Brayton cycles that are the basis for computing the ideal performance of internal combustion and gas turbine engines. The basis of the cycle is the piston-cylinder arrangement (Fig. 13) of elementary thermodynamics. The reactants and explosion products are at all times contained within the cylinder and pistons so that we are always considering a fixed mass. The explosive, pistons, and cylinder will be considered as a closed thermodynamic system. All confining materials are assumed to be rigid, massless, and do not conduct heat. The pistons can be independently moved and there is a work interaction W (> 0 for work done by the system) with the surroundings that results from these motions. In order to have a complete cycle, there will be a heat interaction Q (> 0 for heat transferred into the system) between the system and the surroundings. The piston-cylinder arrangement initially contains reactants at pressure P_1 and temperature T_1.

The steps in the cycle are shown in Fig. 14. The cycle starts with the system at state 1 and the application of external work to move the piston on the left at velocity u_p. It instantaneously initiates a detonation front at the piston surface (step a). The detonation propagates to the right with a velocity U_{CJ} consistent with u_p. The detonation products following the wave are in a uniform state. When the detonation reaches the right piston, it instantaneously accelerates to velocity u_p, and the entire piston-cylinder arrangement moves at constant velocity u_p (step b). The system is then at state 2. The energy of this mechanical motion is converted to external work (step c) by bringing the detonation products to rest at state 3. Then the products are adiabatically expanded to the initial pressure (step d) to reach state 4. Heat is extracted by cooling

†Personal communication from W. C. Davis, April 2003

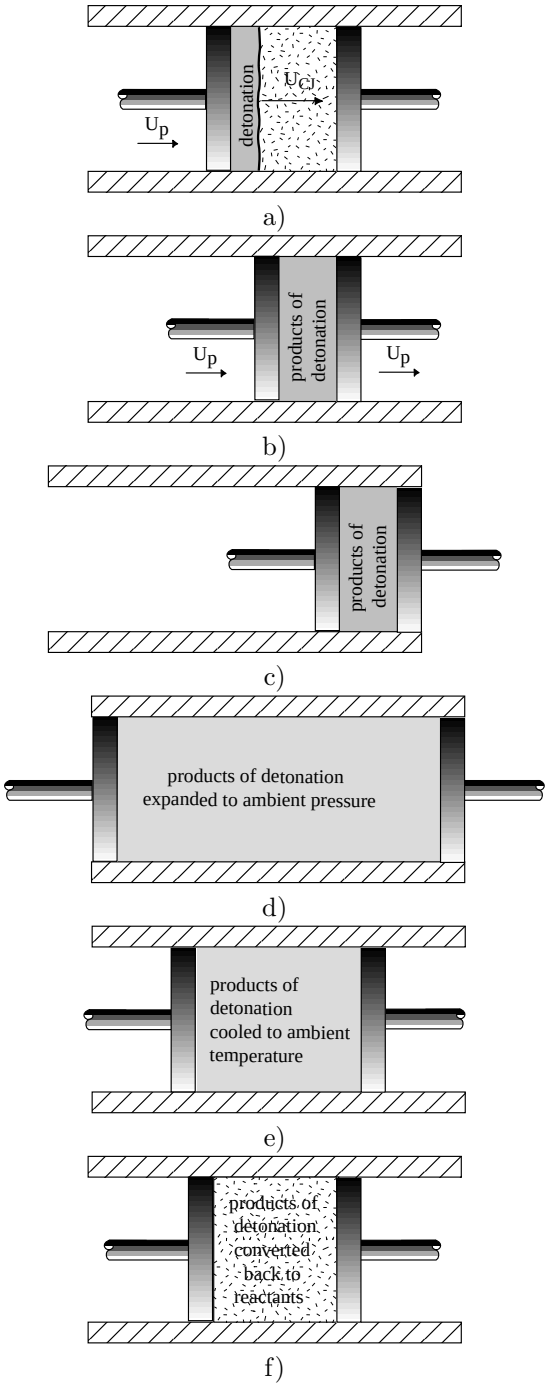

Fig. 14 Physical steps that make up the Fickett-Jacobs cycle. a) Detonation moving to right with simultaneous application of external work to move piston on left at velocity u_p. b) Instantaneous acceleration of piston on right when detonation has consumed all the material. c) Conversion of mechanical motion to external work to bring detonation products to rest. d) Expansion of products back to atmospheric pressure. e) Extraction of energy as heat at constant pressure to return detonation products to initial temperature. f) Conversion of products to reactants at constant temperature and pressure.

the products at constant pressure (step e) to the initial temperature (state 5). Finally, the cycle is completed by converting products to reactants at constant temperature and pressure (step f) and the system reaches state 1.

Based on this sequence of steps, it is possible to calculate the work done by the system. During the detonation part of the cycle (step a), from state 1 to 2, the work received by the system is $W_{12} = -P_2 u_p (t_2 - t_1) A$, since the piston exerts a force P_2 while moving at velocity u_p for a time $t_2 - t_1 = L/U_{CJ}$ required by the wave to propagate across the explosive. Using the fact that $\rho_1 L A$ is the mass $\mathcal{M}$ of the explosive, the work received by the system per unit mass of explosive is

$$w_{12} = -\frac{P_2 u_p}{\rho_1 U_{CJ}} \; . \tag{43}$$

The work done by the system when extracting the energy of the mechanical motion (state 2 to 3) is equal to the kinetic energy of the system. Hence, the work per unit mass of explosive is

$$w_{23} = \frac{u_p^2}{2} \; . \tag{44}$$

The work per unit mass of explosive obtained during the isentropic expansion of the detonation products to initial pressure (state 3 to 4) is

$$w_{34} = \int_3^4 P dv \; . \tag{45}$$

The last steps from state 4 to state 1 involve the exchange of heat and mechanical work used to keep the system at constant pressure. The work per unit mass is

$$w_{41} = P_1 (v_1 - v_4) \; . \tag{46}$$

The net work done by the system is equal to or less than the net work of the cycle $w_{net} = w_{12} + w_{23} + w_{34} + w_{41}$. Hence, w_{net} represents the maximum amount of work that can be obtained from a detonation. The FJ cycle can be represented in a pressure-specific volume diagram (Fig. 15) and w_{net} geometrically represents the area contained within the triangle formed by the state points. Fickett and Davis[13] (p. 35–38) do not account for the work interaction during the process 4–1 in their definition of the net work. They do not consider steps e) and f) to be physical since the detonation products just mix with the surroundings, and they consider the work generated between states 4 and 1 to be "lost" work[‡]. However, these interactions have to be included for consistency with the First Law of Thermodynamics. In high-explosive applications, $P_1 \ll P_2$

[‡]Our first effort[16] to apply the FJ cycle to modeling impulse from detonation tubes used Fickett and Davis' interpretation of the available work rather than the approach taken here. As a consequence, the numerical values of the efficiencies given in Cooper and Shepherd[16] are different than given here.

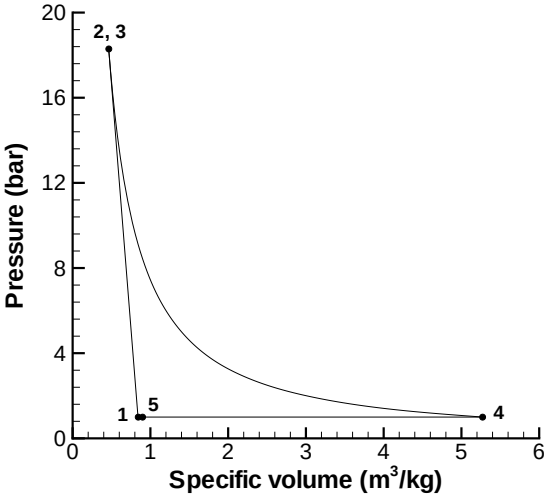

Fig. 15 Pressure-specific volume diagram showing the sequence of states and connecting paths that make up the FJ cycle for a stoichiometric propane-air mixture at 300 K and 1 bar initial conditions.

and the additional work term corresponding to w_{41} may be small compared to the other work terms.

For all steps in the cycle, the First Law of Thermodynamics applies. Using the sign convention defined previously,

$$\Delta E = Q - W \tag{47}$$

where E is the total energy in the system, composed of the internal and kinetic energies. The only heat exchange between the system and the surroundings occurs between steps 4 and 1. Hence, the work done by the system per unit mass of explosive can be calculated for each process as a function of the total energy per unit mass and $w_{14} = e_1 - e_4$. Using Eq. 46, the net work done by the system over the FJ cycle is

$$w_{net} = e_1 - e_4 + P_1(v_1 - v_4) = h_1 - h_4 \; . \tag{48}$$

This result is consistent with Eq. 4 resulting from the general thermodynamic cycle analysis for closed systems undergoing a cycle starting with an arbitrary process between states 1 and 4 and ending with a constant pressure process between states 4 and 1. This consistency is achieved only if w_{41} is included in the computation. It shows that the FJ cycle is a consistent conceptual framework to calculate the amount of work available from a detonation. Since all processes other than the detonation are ideal, the work computed is an upper bound to what can be obtained by any cyclic process using a propagating detonation for the combustion step.

It can be verified using the detonation jump conditions that this result can also be obtained by computing the amount of work done during each individual process. Although it is straightforward from the First Law of Thermodynamics and Eq. 45 that $w_{34} = e_3 - e_4$, it is not obvious that $w_{13} = w_{12} + w_{23} = e_1 - e_3$. We write the detonation wave jump conditions in terms of the velocities in a fixed reference frame.

$$\rho_2(U_{CJ} - u_p) = \rho_1 U_{CJ} \tag{49}$$

$$P_2 = P_1 + \rho_1 U_{CJ} u_p \tag{50}$$

$$h_2 = h_1 - u_p^2/2 + U_{CJ} u_p \tag{51}$$

The work per unit mass generated between states 1 and 3, which correspond respectively to reactants and detonation products at rest, can be calculated using the results of Eqs. 49–51. Note that the thermodynamic properties of states 2 and 3 are identical, but the system at state 3 is at rest whereas it is moving at velocity u_p at state 2. From Eqs. 43 and 44,

$$\begin{aligned} w_{12} + w_{23} &= u_p^2/2 - \frac{P_2 u_p}{\rho_1 U_{CJ}} \\ &= h_1 - h_2 + U_{CJ} u_p - \frac{P_2 u_p}{\rho_1 U_{CJ}} \; . \end{aligned} \tag{52}$$

The third term on the right-hand side of the previous equation can be expressed using Eq. 50, and Eq. 52 becomes

$$w_{12} + w_{23} = h_1 - h_2 + \frac{P_2}{\rho_1}\left(1 - \frac{u_p}{U_{CJ}}\right) - \frac{P_1}{\rho_1} \; . \tag{53}$$

Using the result of Eq. 49, and after some algebra, this equation yields

$$w_{12} + w_{23} = e_1 - e_3 \tag{54}$$

where $e = h - P/\rho$ is the specific internal energy per unit mass of the mixture. Combining this with the previous results, we have

$$w_{net} = w_{12} + w_{23} + w_{34} + w_{41} = h_1 - h_4 \tag{55}$$

in agreement with Eq. 48. Thus, we have verified that our two treatments give identical results. This gives us additional confidence that the FJ physical model of the detonation cycle is correct since the detailed energy balance agrees with the simpler thermodynamic system approach.

Thermal efficiency

The FJ cycle is also used to define a thermal efficiency for the conversion of chemical energy into mechanical work. The thermal efficiency is defined as

$$\eta_{FJ} = \frac{w_{net}}{q_c} = \frac{h_1 - h_4}{q_c} \; . \tag{56}$$

For mixtures with a higher enthalpy at the end of the expansion process (state 4), a higher portion of the useful work is lost through heat transfer during the constant pressure processes between states 4 and 5.

We first investigate the values of the thermal efficiency for a perfect gas model. The detonation process

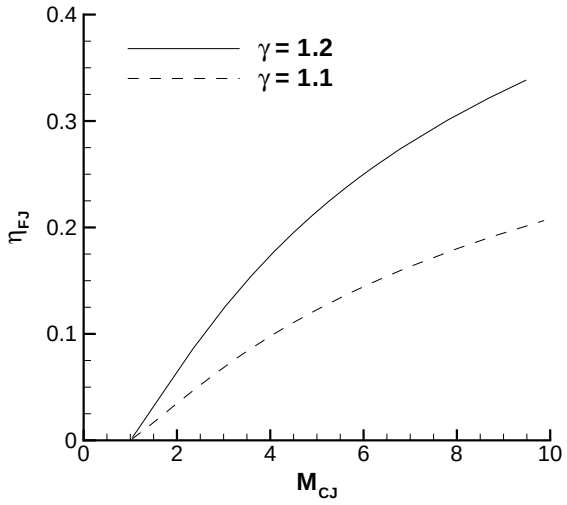

Fig. 16 FJ cycle thermal efficiency as a function of CJ Mach number for the one-γ model of detonation for two values of γ representative of fuel-oxygen ($\gamma = 1.1$) and fuel-air ($\gamma = 1.2$) detonations.

is represented using the one-γ model of detonation[17] for values of γ representative of products from hydrocarbon fuel detonations with oxygen and air. The thermal efficiency for the FJ cycle is calculated for a perfect gas as

$$\eta_{FJ} = 1 - \frac{C_p T_1}{q_c}\left[\frac{1}{M_{CJ}^2}\left(\frac{1+\gamma M_{CJ}^2}{1+\gamma}\right)^{\frac{\gamma+1}{\gamma}} - 1\right]. \tag{57}$$

The FJ cycle thermal efficiency is represented in Fig. 16 as a function of the CJ Mach number for two values of γ representative of fuel-oxygen and fuel-air detonations. The thermal efficiency increases with increasing CJ Mach number, which is itself an increasing function[17] of the heat of combustion q_c. As q_c increases, a lower fraction of the heat released in the detonation process is rejected during the final constant pressure process. In the limit of large M_{CJ}, the thermal efficiency approaches 1 with $1 - \eta_{FJ} \propto (1/M_{CJ}^2)^{1-1/\gamma}$. Looking at the detonation as a ZND process,[13] this result may be interpreted as follows: a higher heat of combustion results in a higher precompression of the reactants through the shock wave before combustion and yields a higher thermal efficiency.

Figure 16 also shows that the variation of the thermal efficiency depends strongly on the value chosen for γ. At constant CJ Mach number, a lower value of γ in the detonation products yields a lower efficiency. The parameter $\gamma - 1$ controls the slope of the isentrope 3–4 in the pressure-temperature plane. Lower values of γ generate lower temperature variations for a fixed pressure ratio P_4/P_3. This means that the temperature at state 4 is higher and the heat rejected during process 4–5 is larger, decreasing the thermal efficiency.

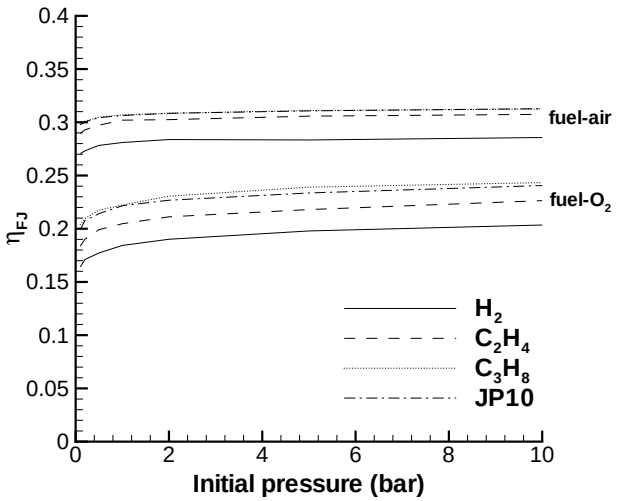

Fig. 17 FJ cycle thermal efficiency for stoichiometric hydrogen, ethylene, propane, and JP10 mixtures with oxygen and air as a function of initial pressure at 300 K.

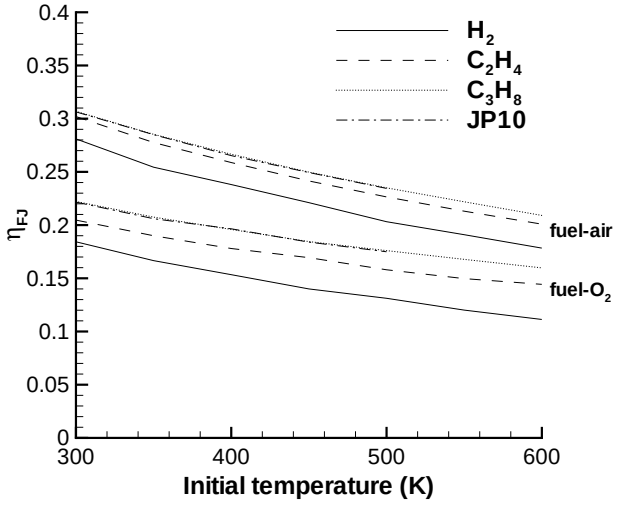

Fig. 18 FJ cycle thermal efficiency for stoichiometric hydrogen, ethylene, propane, and JP10 mixtures with oxygen and air as a function of initial temperature at 1 bar.

The most realistic approach to accounting for property variations is to use fits or tabulated thermochemical properties as a function of temperature for each species and the ideal gas model to find mixture properties. In keeping with the spirit of cycle analysis, all chemical states involving combustion products are assumed to be in equilibrium. The FJ cycle thermal efficiency was calculated using realistic thermochemistry for hydrogen, ethylene, propane, and JP10 fuels with oxygen and air. The equilibrium computations were carried out using STANJAN.[18] The thermal efficiency

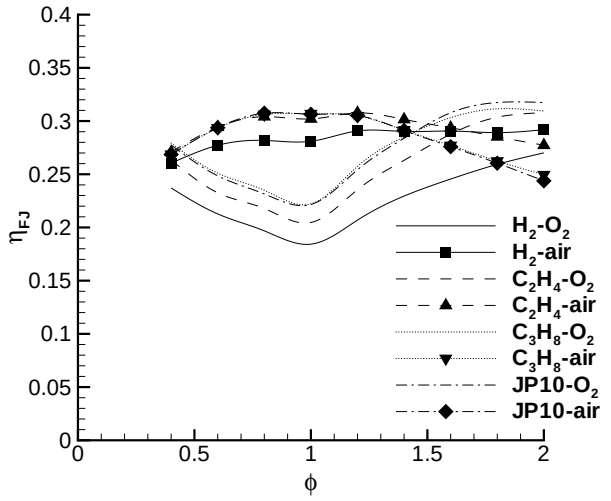

Fig. 19 FJ cycle thermal efficiency as a function of equivalence ratio at 300 K and 1 bar initial conditions for hydrogen, ethylene, propane, and JP10.

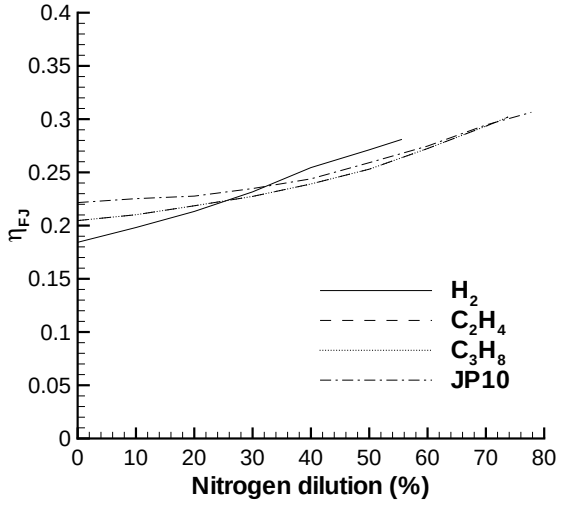

Fig. 20 FJ cycle thermal efficiency as a function of nitrogen dilution for stoichiometric fuel-oxygen mixtures at 300 K and 1 bar initial conditions for hydrogen, ethylene, propane, and JP10.

was determined using Eq. 56. The results are significantly influenced by the variation of the specific heat capacity with temperature in the detonation products and the dissociation and recombination processes.

The thermal efficiency is shown in Fig. 17 as a function of initial pressure. The thermal efficiency decreases with decreasing initial pressure due to the increasing importance of dissociation at low pressures. Dissociation is an endothermic process and reduces the effective energy release through the detonation, and the maximum amount of work that can be obtained from the FJ cycle. Exothermic recombination reactions are promoted with increasing initial pressure and the amount of work generated during the FJ cycle increases. At high initial pressures, the major products dominate and the CJ detonation properties tend to constant values. Thus, the amount of work generated by the detonation and the thermal efficiency asymptote to constant values. Figure 18 shows that η_{FJ} decreases with increasing initial temperature. Because the thermal efficiency is an increasing function of the CJ Mach number (Fig. 16), the decrease in initial mixture density and M_{CJ} caused by the increasing initial temperature[17] is responsible for the decreasing thermal efficiency.

The influence of equivalence ratio on the FJ cycle thermal efficiency is shown in Fig. 19. The trends for fuel-oxygen and fuel-air mixtures are very different. The thermal efficiency for fuel-air mixtures is maximum at stoichiometry, whereas it is minimum for fuel-oxygen mixtures. This behavior illustrates clearly the strong influence of dissociation processes on the thermal efficiency. Fuel-air mixtures generate much lower CJ temperatures than fuel-oxygen mixtures. The effect of dissociation in fuel-air mixtures is weak because a significant part of the energy release is used to heat up the inert gas (nitrogen) and the temperatures are lower than in the fuel-oxygen case. Because of the weak degree of dissociation, these mixtures tend to follow the same trends as the perfect gas and yield a maximum efficiency when the energy release is maximized near stoichiometry. Lean mixtures have very little dissociation and the CJ Mach number increases with the equivalence ratio from 4 to 5 or 6 at stoichiometry. Thus, the thermal efficiency increases with increasing equivalence ratio for $\phi < 1$. Rich mixtures ($\phi > 1$) have significant amounts of carbon monoxide and hydrogen due to the oxygen deficit and the dissociation of carbon dioxide and water, reducing the effective energy available for work and the thermal efficiency.

On the other hand, fuel-oxygen mixtures are characterized by high CJ temperatures, in particular near $\phi = 1$. Endothermic dissociation reactions reduce the effective energy release during the detonation process. During the subsequent expansion process 3–4, the radicals created by the dissociation reactions start recombining. However, the temperature in the detonation products of fuel-oxygen mixtures remains high during this process and only partial recombination occurs. The products at state 4 are still in a partially dissociated state and a significant part of the energy released by the detonation is not available for work. This extra energy is released during the constant pressure process 4–5 under the form of heat and reduces the net work. The influence of this phenomenon increases with increasing CJ temperature, which explains why fuel-oxygen mixtures have a lower efficiency near stoichiometry.

The influence of nitrogen dilution is also investigated

in Fig. 20. The thermal efficiency is plotted as a function of nitrogen dilution for stoichiometric mixtures varying from fuel-oxygen to fuel-air. It increases with increasing nitrogen dilution and is maximum for fuel-air mixtures. This behavior is explained mainly by the influence of dissociation phenomena. The reduction in mixture specific heat capacity with increasing nitrogen dilution also contributes to this behavior.

Although fuel-oxygen mixtures have a higher specific heat of combustion than fuel-air mixtures, Fig. 19 shows that fuel-air mixtures have a higher thermal efficiency, in particular near stoichiometry. This is attributed mainly to dissociation phenomena, but also to the higher value of the effective ratio of specific heats γ in the detonation products of fuel-air mixtures, which results in a higher thermal efficiency (Fig. 16). In general, $1.13 < \gamma_2 < 1.2$ for fuel-oxygen mixtures when varying the equivalence ratio, whereas $1.16 < \gamma < 1.3$ for fuel-air mixtures. The parameter $\gamma - 1$ controls the slope of the isentrope in the pressure-temperature plane. This difference is caused by the influence of recombination reactions in the detonation products. These exothermic reactions are favored in the hot products of fuel-oxygen mixtures, and keep the temperature from dropping as fast as in the colder products of fuel-air mixtures. Note that, although stoichiometric fuel-oxygen mixtures have a lower thermal efficiency than fuel-air mixtures, they generate 2 to 4 times as much work as fuel-air mixtures because of their larger specific heat of combustion.

In general, hydrogen yields the lowest efficiency. Combustion of hydrogen with oxygen produces a mole decrement, which generates a much lower CJ pressure compared to hydrocarbon fuel detonations. Because entropy increases with decreasing pressure, a lower pressure translates into a higher entropy rise and a lower thermal efficiency compared with hydrocarbon fuel detonations. In terms of work done, the work generated during the expansion process w_{34} is much lower for hydrogen detonations because of their lower CJ pressure, which reduces the thermal efficiency. Hydrocarbon fuels have a higher thermal efficiency, with propane and JP10 yielding the highest efficiency. These two fuels have the highest molecular weight of all, which translates into a higher initial density, CJ pressure, and propensity to generate work during the expansion process. The values obtained for the FJ cycle efficiency are quite low, generally between 0.2 and 0.3 for the range of mixtures investigated. The typical way to increase low thermal efficiencies is to precompress the reactants before combustion. The FJ cycle with precompression is investigated next.

FJ cycle with precompression

The role of precompression is to reduce the entropy rise through the combustion process by increasing the initial temperature before combustion.[1] Since entropy increments are detrimental to the thermal efficiency, the most ideal way to increase the fluid temperature is isentropic compression.

The FJ cycle with precompression is based on the steps described in Fig. 14, but it includes an additional process. Before the piston starts moving and initiates the detonation, the reactants are isentropically compressed with the piston to a state 1'. The subsequent sequence of steps is identical to the basic FJ cycle case. The FJ cycle with precompression is represented in Fig. 21 in the pressure-specific volume plane for a propane-air mixture with a precompression ratio of 5. The precompression ratio is defined as $\pi_c = P_{1'}/P_1$.

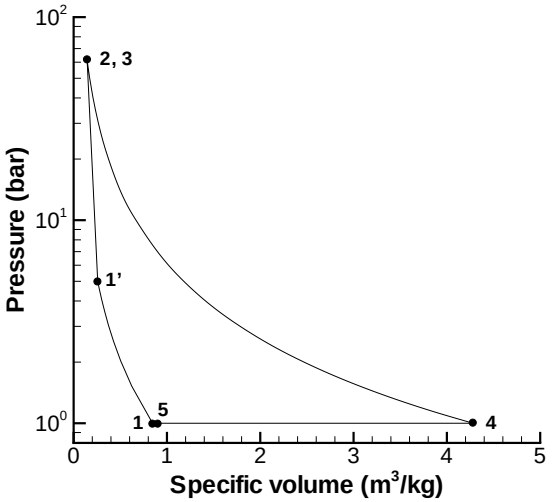

Fig. 21 Pressure-specific volume diagram showing the sequence of states and connecting paths that make up the FJ cycle with precompression ($\pi_c = 5$) for a stoichiometric propane-air mixture at 300 K and 1 bar initial conditions.

During the initial compression of the reactants from state 1 to state 1', the work per unit mass is

$$w_{11'} = -\int_1^{1'} P dv \, . \tag{58}$$

The net work done by the system is then $w_{net} = w_{11'} + w_{1'2} + w_{23} + w_{34} + w_{41}$. Expressions for the terms in the previous equation are given respectively by Eqs. 58, 43, 44, 45, and 46. Applying the First Law of Thermodynamics, the result obtained for the net work $w_{net} = h_1 - h_4$ is identical to that of Eq. 48.

The influence of the compression ratio on the thermal efficiency is investigated first for a perfect gas. The expression for η_{FJ} using the one-γ detonation model is identical to the result of Eq. 57 for the basic FJ cycle. However, in the case of the cycle with precompression, the CJ Mach number varies because of the change in initial temperature before detonation initiation. The thermal efficiency is plotted in Fig. 22 as a function

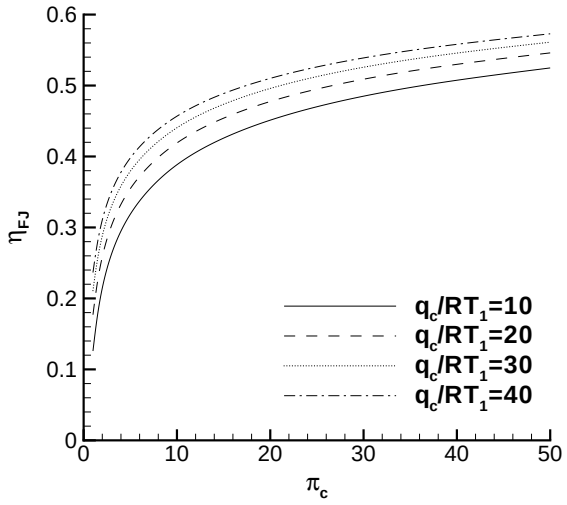

Fig. 22 FJ cycle thermal efficiency as a function of the compression ratio π_c for the one-γ model of detonation using different values of the non-dimensional heat release. $\gamma = 1.2$.

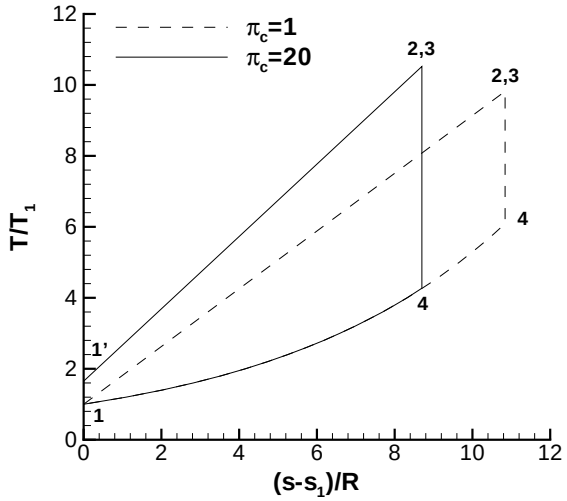

Fig. 23 Temperature-entropy diagram for FJ cycle without and with precompression ($\pi_c = 20$) using the one-γ model of detonation. $q_c/RT_1 = 40$, $\gamma = 1.2$.

of π_c for different values of the non-dimensional energy release. The FJ cycle thermal efficiency increases with increasing compression ratio. This increase can be explained by considering the temperature-entropy diagram of Fig. 23. The heat rejected during the constant-pressure portion of the cycle 4–5 is the area under the temperature-entropy curve between states 4 and 5 (Eq. 9). For a given state 1 and q_{in}, the thermal efficiency is maximized when q_{out} is minimized, which occurs when $s_4 = s_2$ is minimized. Because the total entropy rise decreases with increasing combustion pressure, the cycle thermal efficiency increases with increasing compression ratio. In terms of net work, precompressing the reactants increases the work done during the expansion process (state 3 to 4). The expansion of the hot gases generates more work than is absorbed by the cold gases during the precompression stage, so that precompression increases the thermal efficiency. This idea applies equally well to other types of thermodynamic cycles such as the Brayton or the Otto cycles.

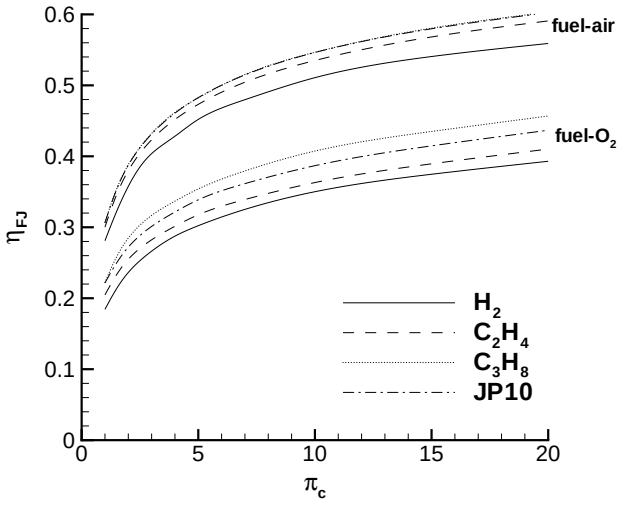

Fig. 24 FJ cycle thermal efficiency as a function of the compression ratio π_c for hydrogen, ethylene, propane, and JP10 with oxygen and air at initial conditions of 1 bar and 300 K.

The result of Eq. 57, which also applies to the FJ cycle with precompression, is identical to the result obtained by Heiser and Pratt[19] in their thermodynamic cycle analysis of pulse detonation engines. They calculated the entropy increments associated with each process in the detonation cycle and formally obtained the same result. However, the numerical values shown in Fig. 22 are lower than those given in Heiser and Pratt[19] due to the difference in the value of the specific heat ratio used. They used a value of $\gamma = 1.4$ corresponding to the reactants, whereas we use values of γ equal to 1.1 or 1.2 since these are more representative of the detonation products. As illustrated in Fig. 16, the value chosen for the specific heat ratio has a strong influence on the results obtained for the thermal efficiency in the one-γ model. A more realistic cycle analysis for a perfect gas involves using the two-γ model of detonations.[17] This approach was applied by Wu et al.,[11] who extended the analysis of Heiser and Pratt[19] to the two-γ model of detonations.

In reality, one- or two-γ models of these cycles cannot correctly capture all the features of dissociation-recombination equilibria and temperature-dependent properties. It is necessary to carry out numerical simulations with a realistic set of product species and properties. Equilibrium computations using realistic thermochemistry were carried out using STANJAN[18]

for hydrogen, ethylene, propane, and JP10. The thermal efficiency is given in Fig. 24 as a function of the compression ratio. Its behavior is similar to the perfect gas case. The influence of dissociation reactions is reduced with increasing compression ratio, but dissociated species are still present for fuel-oxygen mixtures, even for high values of π_c.

Comparison with Brayton and Humphrey cycles

CP combustion is representative of the process undergone by a fluid particle in an ideal ramjet or turbojet engine.[8] Constant-volume (CV) combustion has been used as a convenient surrogate for detonation for the purposes of estimating the thermal efficiency.[20] One viewpoint is that CV combustion is an instantaneous transformation of reactants into products. Another view is that CV combustion is the limit of a combustion wave process as the wave speed approaches infinity.

The ideal Brayton cycle consists of the following processes: isentropic compression, CP combustion, isentropic expansion to initial pressure, and heat exchange and conversion of products to reactants at constant pressure. For the perfect gas, the thermal efficiency of the Brayton cycle depends only on the static temperature ratio across the compression process.[8]

$$\eta_{th} = 1 - \frac{T_1}{T_{1'}} = 1 - \pi_c^{-\frac{\gamma-1}{\gamma}} \tag{59}$$

The Humphrey cycle is similar to the Brayton cycle, except that the combustion occurs at constant volume instead of constant pressure. Unlike the Brayton cycle and like the FJ cycle, the efficiency of the Humphrey cycle also depends on the non-dimensional heat release q_c/CpT_1 and the specific heat ratio γ.

$$\eta_{th} = 1 - \frac{C_p T_1}{q_c}\left[\left(1 + \gamma\frac{q_c}{C_p T_1}\pi_c^{-\frac{\gamma-1}{\gamma}}\right)^{1/\gamma} - 1\right] \tag{60}$$

For fixed energy release and compression ratio, the thermal efficiency of the Humphrey cycle is higher than that of the Brayton cycle, which can be related to the lower entropy rise generated by CV combustion compared with CP combustion (Fig. 5).

Equilibrium computations were carried out using STANJAN[18] to compute the thermal efficiency of the FJ, Humphrey, and Brayton cycles for a stoichiometric propane-air mixture at 300 K and 1 bar initial conditions. The amount of precompression was varied. In comparing different combustion modes, the question of which of the various pressures produced during the combustion event should be considered.[21] Two possibilities are explored here. The first possibility consists of comparing the cycles based on the same pressure before combustion, which corresponds to propulsion systems having equivalent feed systems. The second possibility is based on the peak combustion pressure, which corresponds to propulsion systems designed to operate at the same level of chamber material stresses.

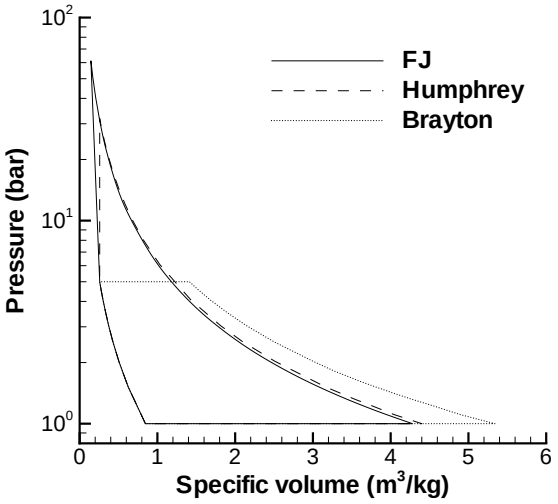

Fig. 25 Pressure-specific volume diagram comparing the FJ, Humphrey, and Brayton cycles with precompression ($\pi_c = 5$) for a stoichiometric propane-air mixture at 300 K and 1 bar initial conditions.

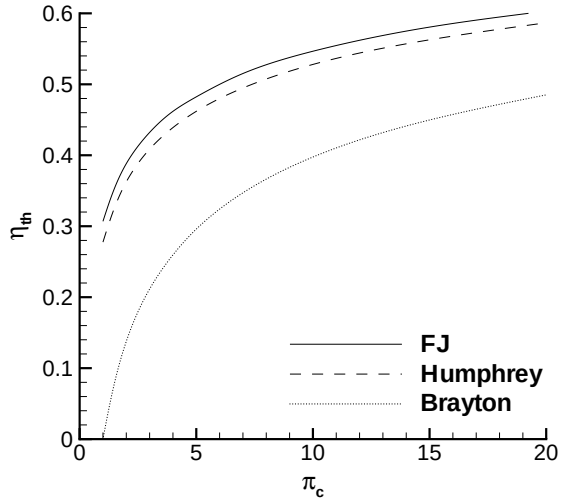

Fig. 26 Thermal efficiency as a function of compression ratio for FJ, Humphrey, and Brayton cycles for a stoichiometric propane-air mixture at 300 K and 1 bar initial conditions.

The cycle efficiencies are shown in Fig. 26 as a function of the compression ratio and in Fig. 27 as a function of the combustion pressure ratio. The combustion pressure ratio π_c' is defined as the ratio of post-combustion pressure to initial cycle pressure. Detonation generates the lowest entropy rise, closely followed by CV combustion and finally CP combustion (Fig. 5). Thus, for a given compression ratio, the FJ cycle yields the highest thermal efficiency, closely fol-

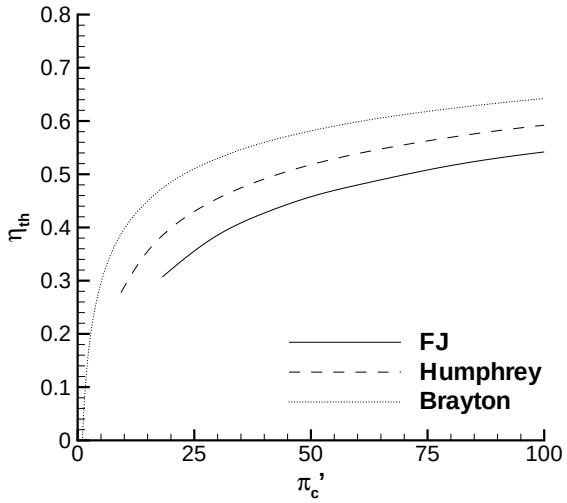

Fig. 27 Thermal efficiency as a function of combustion pressure ratio for FJ, Humphrey, and Brayton cycles for a stoichiometric propane-air mixture at 300 K and 1 bar initial conditions.

lowed by the Humphrey cycle and, finally, the Brayton cycle. This calculation using detailed thermochemistry[18] agrees qualitatively with the thermodynamic cycle analysis results of Heiser and Pratt[19] who used a one-γ model for detonations. The fact that detonation and CV combustion yield very close efficiencies when calculated for the same compression ratio (Fig. 26) has motivated some researchers to estimate pulse detonation engine performance by approximating the detonation process with CV combustion. However, when the thermal efficiency is shown as a function of the combustion pressure ratio (Fig. 27), the trend is inverted and the Brayton cycle yields the highest efficiency, followed by the Humphrey and FJ cycles. The lower efficiency of the FJ cycle can be attributed to the very high peak pressure behind the detonation wave. Although these efficiencies cannot be precisely translated into specific performance parameters, these general results agree with the observations of Talley and Coy[21] based on specific impulse calculations using a gas dynamic model of CV combustion propulsion. The superiority of the Brayton cycle in Fig. 27 will be reduced if the Humphrey and FJ cycles are operated at a higher combustion peak pressure or temperature.

The comparison of the thermal efficiencies in Figs. 26 and 27 shows that unsteady detonations have the potential to generate more mechanical work than CP or CV combustion and, thus, appear to be more efficient combustion process. This result can be directly related to the lower entropy rise associated with detonations. However, as we have already seen for the case of steady detonation, some care is needed in interpreting thermodynamic results in terms of propulsion system performance. We cannot use these efficiencies directly since performance estimates based on Eq. 8 are applicable only to steady propulsion systems. In particular, the initial state (before the detonation wave) and the conversion of thermal energy to impulse in unsteady systems requires detailed consideration of the gas dynamic processes[12] within the engine.

Conclusions

We have used thermodynamic considerations to investigate the merits of detonative combustion relative to other combustion modes for applications in steady and unsteady flow propulsion systems. For steady flow systems, the irreversible component of the entropy rise is shown to control the thermal efficiency. Although detonations generate the minimum amount of total entropy rise along the conventional Hugoniot, they also generate the maximum amount of irreversible entropy rise. For air-breathing propulsion applications, the thermodynamic cycle analysis has to be conducted based on a fixed initial stagnation state. In this case, the total entropy rise for the detonation solutions is much higher than the deflagration solutions and, therefore, engines based on steady detonation have much poorer performance than those based on deflagration. These findings reconcile thermodynamic cycle analysis with flow path performance analysis of detonation-based ramjets.[3–5] The highest thermal efficiency occurs for the combustion process with the lowest entropy increment, corresponding to the ideal Brayton cycle.

For unsteady flow systems, we presented a thermostatic approach of a closed system, the Fickett-Jacobs cycle, to compute an upper bound to the amount of mechanical work that can be produced by a cycle using an unsteady detonation process. This cycle is used to calculate a thermal efficiency based on this ideal mechanical work. Values of the thermal efficiency for a variety of mixtures are calculated for the FJ cycle with and without initial precompression. Fuel-air mixtures are found to have a higher thermal efficiency than fuel-oxygen mixtures near stoichiometry due to dissociation phenomena and to the higher value of the effective ratio of specific heats in their detonation products.

Comparison with the Humphrey and Brayton cycles shows that the thermal efficiency of the FJ cycle is only slightly higher than that of the Humphrey cycle, and much higher than that of the Brayton cycle when compared on the basis of pressure at the start of the combustion process. The opposite conclusion is drawn when the comparison is made on the basis of the pressure after the combustion process. Although these efficiencies cannot be precisely translated into propulsive efficiency, these results are useful in comparing unsteady detonation with other combustion modes.

Acknowledgments

This work was supported by Stanford University Contract PY-1905 under Dept. of Navy Grant No. N00014-02-1-0589 "*Pulse Detonation Engines: Initiation, Propagation, and Performance*".

References

[1]Foa, J. V., *Elements of Flight Propulsion*, John Wiley & Sons, New York, 1960.

[2]Courant, R. and Friedrichs, K. O., *Supersonic Flow and Shock Waves*, Interscience Publishers, Inc., New York, 1967.

[3]Dunlap, R., Brehm, R. L., and Nicholls, J. A., "A Preliminary Study of the Application of Steady-State Detonative Combustion to a Reaction Engine," *Jet Propulsion*, Vol. 28, No. 7, 1958, pp. 451–456.

[4]Sargent, W. H. and Gross, R. A., "Detonation Wave Hypersonic Ramjet," *ARS Journal*, Vol. 30, No. 6, 1960, pp. 543–549.

[5]Wintenberger, E. and Shepherd, J. E., "The Performance of Steady Detonation Engines," *submitted to Journal of Propulsion and Power*, 2003, also AIAA 2003-0714.

[6]Clarke, J. M. and Horlock, J. H., "Availability and Propulsion," *Journal of Mechanical Engineering Science*, Vol. 17, No. 4, 1975, pp. 223–232.

[7]Riggins, D. W., McClinton, C. R., and Vitt, P. H., "Thrust Losses in Hypersonic Engines Part 1: Methodology," *Journal of Propulsion and Power*, Vol. 13, No. 2, 1997, pp. 281–287.

[8]Oates, G. C., *Aerothermodynamics of Gas Turbines and Rocket Propulsion*, AIAA Education Series, 1984.

[9]Foa, J. V., "Single Flow Jet Engines - A Generalized Treatment," *Journal of the American Rocket Society*, Vol. 21, 1951, pp. 115–126.

[10]Kailasanath, K., "Review of Propulsion Applications of Detonation Waves," *AIAA Journal*, Vol. 38, No. 9, 2000, pp. 1698–1708.

[11]Wu, Y., Ma, F., and Yang, V., "System Performance and Thermodynamic Cycle Analysis of Airbreathing Pulse Detonation Engines," *Journal of Propulsion and Power*, Vol. 19, No. 4, 2003, pp. 556–567.

[12]Wintenberger, E. and Shepherd, J. E., "A Model for the Performance of Air-Breathing Pulse Detonation Engines," *submitted to Journal of Propulsion and Power*, 2003, also AIAA 2003-4511.

[13]Fickett, W. and Davis, W. C., *Detonation Theory and Experiment*, Dover Publications Inc., 2001.

[14]Jacobs, S. J., "The Energy of Detonation," NAVORD Report 4366, U.S. Naval Ordnance Laboratory, White Oak, MD. Available as NTIS AD113271 – Old Series.

[15]Zel'dovich, Y. B., "On the Use of Detonative Combustion in Power Engineering," *Journal of Technical Physics*, Vol. 10, No. 17, 1940, pp. 1453–1461, in Russian.

[16]Cooper, M. and Shepherd, J. E., "The Effect of Nozzles and Extensions on Detonation Tube Performance," 38th AIAA/ASME/SAE/ASEE Joint Propulsion Conference and Exhibit, July 7-10, 2002, Indianapolis, IN, AIAA 2002-3628.

[17]Thompson, P. A., *Compressible Fluid Dynamics*, Advanced Engineering Series, Rensselaer Polytechnic Institute, pp. 347–359, 1988.

[18]Reynolds, W., "The Element Potential Method for Chemical Equilibrium Analysis: Implementation in the Interactive Program STANJAN," Tech. rep., Mechanical Engineering Department, Stanford University, 1986.

[19]Heiser, W. H. and Pratt, D. T., "Thermodynamic Cycle Analysis of Pulse Detonation Engines," *Journal of Propulsion and Power*, Vol. 18, No. 1, 2002, pp. 68–76.

[20]Bussing, T. R. A. and Pappas, G., "Pulse Detonation Engine Theory and Concepts," *Progress in Aeronautics and Astronautics*, Vol. 165, AIAA, 1996, pp. 421–472.

[21]Talley, D. and Coy, E., "Constant Volume Limit of Pulsed Propulsion for a Constant Gamma Ideal Gas," *Journal of Propulsion and Power*, Vol. 18, No. 2, 2002, pp. 400–406.